On the Constitution of Sodium at Higher Densities

J. B. Neaton* and N. W. Ashcroft

Laboratory of Atomic and Solid State Physics and Cornell Center for Materials Research, Cornell University,
Ithaca, New York 14853-2501

(Received 30 October 2000)

Using density functional theory the atomic and electronic structures of sodium are predicted to depart substantially from those expected of simple metals for $r_s < 2.48$ ($p > 130$ GPa). Newly predicted phases include those with low structural symmetry and semimetallic electronic properties (including zero-gap semiconducting limiting behavior), and even those that raise the possibility of superconductivity, all at currently achievable pressures. Important differences emerge between sodium and lithium at high densities, and these are attributable to corresponding differences in their respective cores.

DOI: 10.1103/PhysRevLett.86.2830 PACS numbers: 61.50.Ks, 71.20.Dg

In their classic papers, *On the Constitution of Metallic Sodium,* Wigner and Seitz [1] successfully described ground state properties of sodium invoking the notion of a nearly free electron metal, one whose valence electrons are only weakly perturbed by an underlying periodic arrangement of ions. An assumption central to their conclusions (and important to the developing concept of the *simple metal*) was that the tightly bound core electrons remain largely unaltered with respect to those in the free atom. At its stabilizing (atmospheric) density, this assumption is valid because the ion cores occupy an exceedingly small fraction of the overall volume of the solid. But, as we show in this Letter, if the overall density (and hence relative core volume) is increased by pressures that are currently achievable, the core states come in to play and the electronic structure of sodium departs quite significantly from this simple metal paradigm.

Recently it was predicted [2] that the ground state of steadily compressed lithium, also a prototypical "simple" metal, would be unstable to less symmetric, *semimetallic* structures beginning at pressures near 50 GPa; and, remarkably, it was suggested that the tendency towards less metallic behavior with increasing pressure would culminate in a nearly insulating, *paired* ground state [2] at about 100 GPa. Two groups, using diamond-anvil cells, have since reported that lithium gradually loses its Drude-like luster under compression, first becoming grey and then finally black (i.e., strongly absorbing) at about 50 GPa [3,4]. Another group, using dynamical shock methods, observed a declining conductivity with increasing density [5], broadly consistent with these results. Recent structural measurements (and associated first-principles calculations) by Hanfland *et al.* [6] find a complex cubic, 16-atom unit cell with space group $I\bar{4}3d$ in lithium near 50 GPa and 200 K. Interestingly enough, although Ref. [6] reports a decline in reflectivity against diamond, it is suggested that the general characteristics remain notably metallic. Although the possibility of broken electronic symmetry states in the light alkalis has been raised earlier [7], such states are of a very different physical character from what is now being found, especially as we show for sodium.

The striking departure from the simple, nearly free electronlike behavior conventionally associated with lithium under standard conditions is attributed in Ref. [2] to an electron-ion interaction (or pseudopotential) which, on the length scales of relevance, becomes increasingly repulsive with density; it originates with the combined effects of Pauli exclusion and orthogonality. Given the novel structural and electronic properties predicted to result from these growing effects under compression, it is natural to examine the stability of other metals at higher densities often regarded as "simple." In this Letter we report results of first-principles calculations, indicating that some low-coordinated structures first predicted for lithium [2,6] are also found to be favored in sodium beginning near 130 GPa. Further, as in lithium, these unexpected transitions are accompanied by significant departures from nearly free electronlike behavior and should be accessible through optical response. Differences in the cores of lithium and sodium result in complementary differences in ground state atomic and electronic structures; yet sodium is also predicted to finally take up the paired *Cmca* phase with nearly zero-gap semiconducting electronic properties.

To study the structural and electronic behavior of sodium over a wide range of densities, we use a plane-wave implementation [8] of density functional theory within the local-density approximation (LDA) [9] and the projector-augmented wave (PAW) method [10,11]. Hellmann-Feynman forces are calculated, and the ions are steadily relaxed to equilibrium positions; all lattice vectors are optimized at constant volume. As the equation of state will be affected by increasing core overlap at high densities, we treat the $3s$, $2p$, and $2s$ electrons as a valence and incorporate only the tightly bound $1s$ state into an effective frozen core. Previous first-principles calculations of standard low- and high-pressure structural and electronic properties of dense sodium [12–15] appear to be limited to the monatomic lattices bcc, fcc, and hcp. Experimentally it is well known that sodium undergoes a martensitic transformation below 35 K, possibly to the $9R$ phase (as in lithium) [16], illuminating the role of dynamics in its stabilization at one atmosphere; our static calculations predict that hcp is very slightly favored over bcc, fcc, and also 9*R* at one atmosphere, but by energies less than 1 meV/ion (quite small compared with dynamical energies and about equal to the accuracy of our calculations) and consistent with previous work [14]. The equilibrium density we calculate for Na in both the fcc and bcc structures ($r_s = 3.78$) is also in excellent agreement with previous LDA results [13,14], overestimating that found in experiment ($r_s = 3.93$ [17]) by slightly more than 10%. [Here $r_s = (3V/4\pi N_e)^{1/3}$, where V is the volume (a.u.^{3}) per ion and N_e corresponds to one electron/atom throughout.] Above 5 GPa the bcc structure emerges with lowest enthalpy, but, after an additional 3-fold reduction in volume to $r_s = 2.66$ ($p = 71$ GPa), we find that bcc is actually unstable to fcc, again consistent with the results of a previous study [15].

Under atmospheric conditions, the ground state electronic structure of sodium therefore conforms to the classic nearly free electron system of Wigner and Seitz [1], having a single valence electron and an equilibrating density where the core volume is certainly an exceedingly small fraction of the cell volume. The pseudopotential for sodium at this density is quite well approximated as local, and under moderate compression a purely local picture also continues to suffice: The primary Fourier component of the pseudopotential V_G diminishes relative to the growing bandwidth. But beyond an approximately 3-fold compression in volume this simple interpretation no longer holds. In Fig. 1 we plot the band structure of fcc sodium at $r_s = 2.3$ and compare it with that of lithium at the same density. The bands near points K, W, and L of Na are quite different from those of Li, and, interestingly, the Fermi surface does remain nearly spherical in Na at these elevated densities. Further, the local density of states (LDOS) of Na has a growing d character; in Li, only s character and p character are observed at $r_s = 2.3$ [19,20]. However, despite these differences, both exhibit sizable gaps at X and, in contrast to the predictions of the nearly free electron model, these gaps are now noticably *growing* in magnitude with increasing density.

For lithium the departure from nearly free electron behavior has evidently been predicted to result in relatively low-coordinated and open atomic structures [2,6]. Likewise for sodium when the same non-Bravais lattices are considered, we find that it is also unstable to the formation of these *lower-coordinated* phases for densities greater than $r_s = 2.48$. A plot of their enthalpies versus pressure appears in Fig. 2. The newly observed cubic $I\bar{4}3d$ phase in lithium [6] is also found to be favored over fcc in Na at $p \sim 130$ GPa ($\sim$3.5-fold compression): In it, each sodium atom has essentially eleven neighbors (three at a distance of 2.15 Å, two at 2.23 Å, and six at 2.39 at a

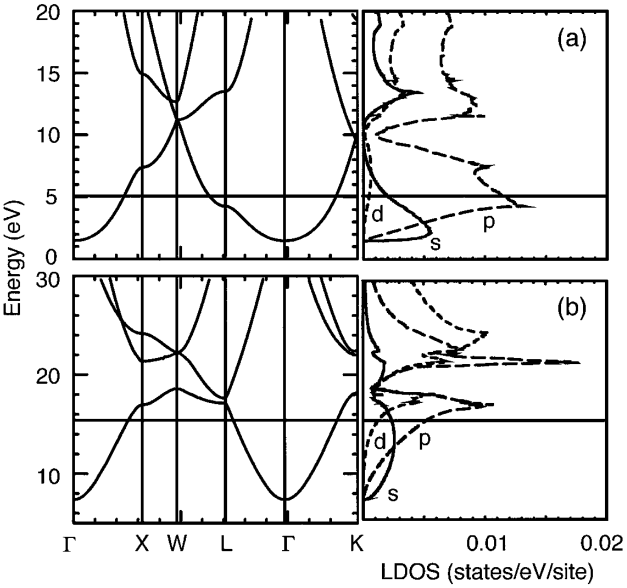

FIG. 1. Band structures, and s, p, and d local densities of states at $r_s = 2.3$ for fcc (a) lithium ($p \sim 60$ GPa) and (b) sodium ($p \sim 245$ GPa). Solid horizontal lines denote the Fermi energies. The free electron value for the Fermi energy at this density is 9.47 eV. The 2s and 2p bandwidths in sodium at this density are 1.25 and 3.5 eV, respectively; the 1s bands in lithium are 0.7 eV wide.

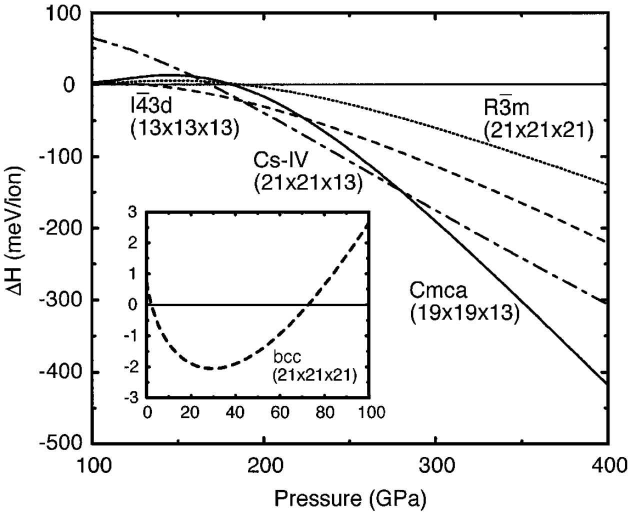

FIG. 2. Enthalpy difference $H - H_{\mathrm{fcc}}$ (meV) vs pressure p (GPa) for competitive structures of dense Na. The inset illustrates the calculated low-pressure bcc-fcc transition described in the text. The *A*7, *Fmmm*, simple cubic, β-Sn, and 9*R* phases (all lower in enthalpy than fcc above 250 GPa but uncompetitive with *Cmca*) are omitted from the figure for clarity. $R\bar{3}m$ is the space group of the primitive rhombohedral phase (see [6]). The Monkhorst-Pack **k** meshes appear in the legend and resulted in the convergence of the total energy to $\sim$1 meV/ion. For densities below $r_s = 2.4$ we use a PAW potential with a 37 Ry plane-wave cutoff and a maximum core radius of 1.16 Å; for the highest densities we use a potential having a 90 Ry cutoff and maximum core radius of 0.76 Å. (Results at low densities are independent of the potential.) $E(V)$ is well fit to $\sum_{n=-2}^{2} a_n V^{n/3}$. Previous static compressions of Na reached only 30 GPa [18].

density of $r_s = 2.4$) [21]. Before reaching $r_s = 2.3$, however, our calculations predict that sodium should transform to Cs-IV at $p \sim 190$ GPa ($r_s = 2.32$). The Cs-IV phase, in which each ion is coordinated by four others [22], can be obtained by a tetragonal distortion of the diamond structure along [001]. Finally, for densities above $r_s = 2.24$ ($p \sim 280$ GPa), a transition to *Cmca* is predicted, and we find this phase to be favored to the highest pressures allowed by our PAW potentials ($p \sim 900$ GPa). In each 8-atom orthorhombic cell of *Cmca*, two *pairs* of ions lie in two distinct adjacent (100) planes displaced with respect to one another by half of a lattice vector in the [010] direction [23]. These predictions are clearly limited by our choice of structures, and for this reason experiment will again play a crucial role (as in lithium [6]). It is clear from Fig. 2, however, that simple, monatomic structure are not stable above 130 GPa [15]. Going beyond LDA we find that gradient corrections [24] result in an expanded equilibrium volume and shift the Cs-IV to *Cmca* transition to ~260 GPa, but do not change transition pressures at lower densities. In addition, spin polarization effects are found to be insignificant.

Sodium remains metallic in both the $I\bar{4}3d$ and Cs-IV phases, and notably the transition into each is accompanied by additional shifts of p and d states below the Fermi energy. The Cs-IV phase was not predicted to precede the *Cmca* phase in lithium, and the difference here may be understood by observing that the d states descend under compression in sodium (as in dense Cs [25]) but not in lithium [20]. Once in *Cmca*, sodium becomes increasingly less metallic as the density rises; the total and local DOS are plotted in Fig. 3 for the predicted *Cmca* phase near the highest density achieved, and most strikingly, at these extremely high pressures (above 800 GPa), sodium, as with lithium before it, approaches a zero-gap semiconducting phase despite considerable differences in core physics. As a direct result of the minimal DOS at the Fermi energy, dense sodium should become increasingly absorbing in the visible, and its resistivity should increase dramatically [26]. Once again the combined effects of Pauli exclusion and orthogonality result in an increasing valence electron density in the *interstitial* regions with density; we observe that the valence charge density in $I\bar{4}3d$, Cs-IV, and *Cmca* is *minimal near and between the ions* (in regions of maximum core overlap) and *maximal in the interstitial regions* [27]: The valence electrons are evidently forced away from the cores (and regions of significant core overlap, i.e., the regions between neighboring ions) into the roomier interstitial space, resulting in significant benefits for both kinetic and exchange energies.

The exclusionary effects mentioned above, arising from core overlap, and also the nature of the cores themselves, strongly influence the atomic and electronic structures of compressed sodium, which we find to have growing p and d character with density. At low densities large kinetic energy costs prevent these bands from dropping below the Fermi energy. But at higher densities rising core overlap will favor less symmetric charge distributions, and the associated Bloch wave functions have an angular momentum character that depends on the details of the core itself. Sodium's core, for example, contains both s and p states. Bloch states with these angular momentum components (i.e., $3s$ and $3p$) are largely excluded from the core region (where their attraction to the bare nuclear potential $-11e/r$ is greatest), raising their electrostatic energy. Bloch states with d character in sodium (and p character in lithium, as its core contains only the $1s$ state), however, *are* able to sample the full nuclear potential. (The more asymmetric $3p$ states in sodium will also have a relatively lower kinetic energy at these densities because of core *overlap,* and therefore continue to be important as well.) Thus in sodium the $3d$ bands rapidly drop and increasingly hybridize with the $3p$ bands under sufficient compression, even though they remain nominally above the unoccupied $3p$ bands at normal densities. Similarly the $2p$ bands descend in lithium [19,20] because they are absent from its core.

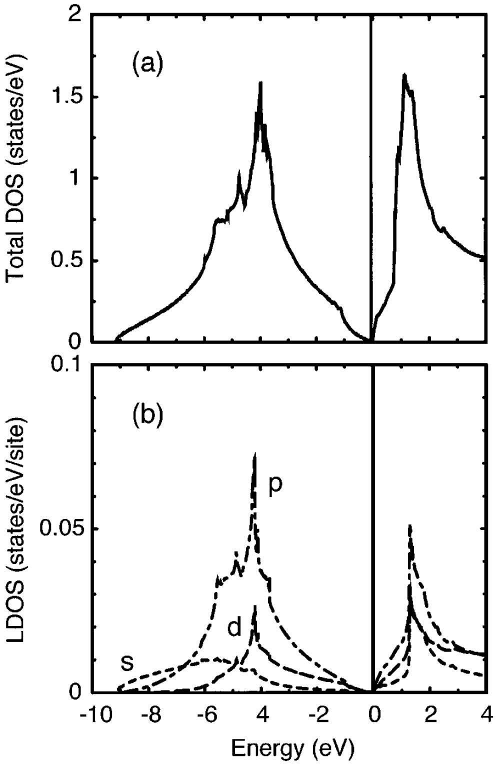

FIG. 3. Valence band (a) total and (b) local density of states of Na in the *Cmca* structure at $r_s = 1.9$ (~880 GPa). The partial wave l character of the DOS is primarily p, but there is also a significant amount of d character which is growing with increasing density. At lower pressures ($p \sim 300-600$), the DOS also exhibits a minimum at the Fermi energy (though it is not zero, as it nearly is above); the state density at the Fermi energy is found to steadily decline with increasing pressure. A solid black vertical line denotes the Fermi energy. The l-projected LDOS is determined within a 0.75 Å sphere.

We have seen here that at the relevant length scales the electron-ion interaction in sodium is no longer weak under compression (again as in lithium), and its putative "simple" metallic behavior at low densities appears to be an accident of the relative core and unit cell volumes present at one atmosphere. Whether exclusionary effects actually culminate in an eventual transition to an insulating state [7] in sodium remains to be resolved by future experiments. Since the interstitial charge buildup is a consequence of general quantum mechanical arguments, the underlying effects revealed here should be evident in other elements and compounds under sufficiently large compressions. In addition, the dramatic changes in the atomic and electronic structure revealed here and in Ref. [2] indicate a large electron-phonon interaction, enhancing the possibility for observation of a significant superconducting transition temperature (a possibility also noted for lithium in Ref. [2] for both monatomic and paired phases). Recent estimations [28] suggest the possibility of large transition temperatures for dense lithium, but a rigorous treatment of electron-electron interactions (necessary for single-band lithium at normal pressures [29]) remains to be performed and may substantially affect the predicted transition temperatures [29]. Finally the effects of temperature on the structural transformations predicted here will also be a matter of considerable experimental interest.

We acknowledge K. Syassen and N. E. Christensen for communicating results prior to publication, and we thank M. P. Teter and A. Bergara for useful discussions. We are indebted to G. Kresse for generating the PAW potentials and, with J. Hafner, for also providing the VASP code. This work was supported by the National Science Foundation (DMR-9988576). This work made use of the Cornell Center for Materials Research Shared Experimental Facilities, supported through the National Science Foundation Materials Research Science and Engineering Centers Program (DMR-0079992).

---

*Present address: Department of Physics and Astronomy, Rutgers University, Piscataway, New Jersey 08854.

[1] E. Wigner and F. Seitz, Phys. Rev. **43**, 804 (1933); *ibid.* **46**, 509 (1934).
[2] J. B. Neaton and N. W. Ashcroft, Nature (London) **400**, 141 (1999).
[3] V. V. Struzhkin, R. J. Hemley, and H. K. Mao, Bull. Am. Phys. Soc. **44**, 1489 (1999).
[4] Y. Mori and A. Ruoff, Bull. Am. Phys. Soc. **44**, 1489 (1999).
[5] V. E. Fortov *et al.,* JETP Lett. **70**, 628 (1999).
[6] M. Hanfland, K. Syassen, N. E. Christensen, and D. L. Novikov, Nature (London) **408**, 174 (2000).
[7] F. Siringo, R. Pucci, and G. G. N. Angilella, High Press. Res. **15**, 255 (1997).
[8] All calculations are performed with the Vienna *ab initio* Simulations Package (VASP). See G. Kresse and J. Furthmüller, Comput. Mater. Sci. **6**, 15 (1996); G. Kresse and J. Furthmüller, Phys. Rev. B **54**, 11 169 (1996).
[9] P. Hohenberg and W. Kohn, Phys. Rev. **136**, 864B (1964); W. Kohn and L. J. Sham, Phys. Rev. **140**, 1133A (1965).
[10] P. Blöchl, Phys. Rev. B **50**, 17 953 (1994).
[11] G. Kresse and D. Joubert, Phys. Rev. B **59**, 1758 (1999).
[12] A. K. McMahan and J. A. Moriarty, Phys. Rev. B **27**, 3235 (1983).
[13] See J. E. Jaffe, Z. Lin, and A. C. Hess, Phys. Rev. B **57**, 11 834 (1998), and references therein.
[14] M. M. Dacorogna and M. L. Cohen, Phys. Rev. B **34**, 4996 (1986).
[15] M. I. Katsnelson *et al.,* Phys. Rev. B **61**, 14 420 (2000).
[16] C. S. Barrett, Acta Crystallogr. **9**, 671 (1956); O. Blaschko *et al.,* Phys. Rev. B **59**, 9095 (1999).
[17] S. N. Vaidya, I. C. Gettings, and G. C. Kennedy, J. Phys. Chem. Solids **32**, 2545 (1971).
[18] I. V. Aleksandrov *et al.,* JETP Lett. **36**, 411 (1983).
[19] J. C. Boettger and S. B. Trickey, Phys. Rev. B **32**, 3391 (1985).
[20] W. G. Zittel *et al.,* J. Phys. F **15**, L247 (1985).
[21] The $I\bar{4}3d$ phase is related to bcc by an internal parameter x [6], which we find to vary from 0.03 at $r_s = 2.5$ to 0.057 at $r_s = 2.3$ (the bcc value being $x = 0$).
[22] The axial (c/a) ratios of Cs-IV vary between $(r_s = 2.4)$ and 2.91 $(r_s = 2.2)$. Large c/a ratios in this structure have been observed before in dense Cs. See K. Takemura, S. Minomura, and O. Shimomura, Phys. Rev. Lett. **49**, 1772 (1982).
[23] The *Cmca* structure has a 4-atom (i.e., two pairs) *primitive* cell. See, e.g., W. B. Waeber, J. Phys. C **2**, 882 (1969). The primitive cell was doubled in a preliminary stability check; we reserve larger unit cells for future work. The structural parameters found here in Na differ considerably from those previously found in Li [2,6]. Besides the lone neighbor, the ions in *Cmca* have two other second neighbors only 5% farther away and four third neighbors 11% farther away. The c/a ratio is found to decrease from 1.38 at $r_s = 2.2$ to 1.15 at $r_s = 1.9$.
[24] J. P. Perdew *et al.,* Phys. Rev. B **46**, 6671 (1992).
[25] R. Sternheimer, Phys. Rev. **78**, 235 (1950); S. G. Louie and M. L. Cohen, Phys. Rev. B **10**, 3237 (1974); A. K. McMahan, Phys. Rev. B **29**, 5982 (1984).
[26] D. Sherrington and W. Kohn, Phys. Rev. Lett. **21**, 153 (1968).
[27] J. B. Neaton, Ph.D. thesis, Cornell University, 2000.
[28] N. E. Christensen and D. L. Novikov, Phys. Rev. Lett. **86**, 1861 (2001).
[29] C. F. Richardson and N. W. Ashcroft, Phys. Rev. B **55**, 15 130 (1997).